[CANCER RESEARCH 63, 6674–6679, October 15, 2003]

Loss of p53 Has Site-Specific Effects on Histone H3 Modification, Including Serine 10 Phosphorylation Important for Maintenance of Ploidy[1]

Simon J. Allison and Jo Milner[2]

Yorkshire Cancer Research p53 Research Group, Department of Biology, University of York, York YO10 5DD, United Kingdom

ABSTRACT

Histone modification enables the ordered regulation of DNA-related processes. Here, we ask if p53, which interacts with histone modifying complexes *in vivo*, influences histone H3 modification. For this purpose, we compared isogenic clones of human p53+/+ and p53−/− cells in which it is reasonable to attribute any observed differences in histone modification to p53-related effects. Cell growth and cell cycle analyses indicated equivalent proliferation rates for the p53+/+ and p53−/− cell clones. Modification of histone H3 was determined under normal cell growth conditions and also after UV irradiation and/or treatment with trichostatin A (TSA) or nicotinamide (two inhibitors of histone deacetylation). Site-specific histone H3 modifications were determined by immunoblotting. We provide evidence that p53 influences histone H3 acetylation at lysine 9 (K9) and K14, whereas acetylation of K18 appears to be p53 independent. The most striking p53-related effects are at K9, which is underacetylated in p53−/− cells under normal conditions of growth but which shows a dramatic increase in acetylation after combined treatment with UV plus TSA. Conversely, phosphorylation of serine 10 (S10P) is elevated in p53−/− cells and reduced after UV plus TSA treatment. Similar reciprocity between K9Ac and S10P was not evident in p53+/+ cells. Abnormal S10P in p53−/− cells was also observed under completely different experimental conditions where cells were treated with nocodazole to induce G_2-M arrest and elevation of S10P (which is linked with G_2-M of the cell cycle). On removal of nocodazole, the p53+/+ cells exhibited rapid reduction in S10P levels and cell cycle recovery. In contrast, the p53−/− cells retained elevated S10P levels and failed to show normal cell cycle recovery. Phosphorylation of S10 is known to be linked with the initiation of chromosome condensation in G_2 and is also important for proper chromosome segregation at mitosis. Our results indicate that loss of p53, directly or indirectly, perturbs the normal regulation of S10 phosphorylation. We suggest that this effect may contribute toward the development of abnormal chromosomes and aneuploidy in p53-deficient cancers.

INTRODUCTION

The tumor suppressor p53 is a multifunctional protein essential for maintenance of genomic integrity in mammalian cells (1). In response to DNA damage, p53 governs the expression of genes necessary for DNA repair and cell growth arrest and apoptosis (see Ref. 2 for bibliography). p53 also enables global chromatin relaxation necessary for nucleotide excision repair of DNA adducts caused by UV irradiation and environmental carcinogens (2). Both gene transactivation and DNA repair require histone acetylation and, as expected, acetylation increases after UV irradiation (3). Previously, we have noted abnormally low levels of histone H3 acetylation in p53-deficient human fibroblasts and human epithelial cells (2). Prompted by this observation, we have now explored the relationship between p53 and cellular histone H3 modifications under normal conditions of cell growth and also in response to UV irradiation, which activates p53 as a transcription factor. Isogenic clones of p53+/+ and p53−/− cells (4) were used in which it is reasonable to attribute any differences in histone modifications to p53-related effects.

For lysine 9 (K9), we show that both constitutive and UV-induced acetylation levels are p53 dependent. K14 acetylation levels are also UV responsive with p53-dependent kinetics. In contrast, K18 acetylation appears p53 independent and invariant. Phosphorylation at serine 10 occurs at mitosis and, as expected, was unaffected either by UV irradiation or by treatment with TSA, an inhibitor of histone deacetylation; loss of p53, however, was associated with marked abnormalities in S10 phosphorylation, with between 2- and 4-fold higher levels compared with p53+/+ cells under normal growth conditions.

S10 phosphorylation of histone H3 is important not only for transcriptional regulation (reviewed in Ref. 5) but also for chromosomal condensation in G_2 of the cell cycle and for proper chromosome segregation at mitosis (6–10). Accumulating evidence (reviewed in Ref. 11) supports the concept that aneuploidy is a key factor in the process of malignant transformation, and histone H3 S10 phosphorylation appears to be involved (12). In our present study, a decrease in S10P levels was observed after treatment with TSA. This unexpected effect of TSA on S10 phosphorylation was specific for p53−/− cells and inversely correlated with stabilization of K9 acetylation levels in response to TSA. Such effects may contribute toward the known anticancer properties of histone deacetylation inhibitors *in vivo*. Abnormal S10 phosphorylation was also observed after the release of p53−/− cells from nocodazole-induced G_2-M cell growth arrest and correlated with impaired cell cycle recovery.

MATERIALS AND METHODS

Cell Culture. HCT116 p53+/+ and HCT116 p53−/− epithelial cells (4), derived from a human colorectal carcinoma, were grown in DMEM with 10% FCS, 2 mM glutamine, 100 units/ml penicillin, and 100 μg/ml streptomycin at 37°C in 5% CO_2 in air.

UV Irradiation and Treatment of Cells with TSA and Nicotinamide. For UV irradiation and TSA experiments, parallel cultures were seeded in 100-mm dishes at 2.5×10^6 cells/dish. After 24 h, TSA was added to the relevant dishes at a final concentration of 500 nM. After an additional 20 h, some of the cells were UV irradiated as follows: culture medium was removed, and cells were washed with PBS and exposed to UV irradiation from a UV-C tube at 10 J/m^2. Culture media were replaced (containing TSA where present previously), and cells returned to 37°C in a 5% CO_2 atmosphere. Cells were harvested for analysis at 20, 40, and 60 min after UV irradiation, and untreated controls were included in every experiment, *i.e.*, post-TSA treatment/no treatment and/or UV irradiation. For treatment with nicotinamide, exponentially growing cells were treated with 5 mM nicotinamide for 2 h before harvesting and immunoblotting. Controls included untreated cells and cells treated for 2 h with 500 nM TSA. The effect of overnight treatment (20 h) with 1, 5, and 20 mM nicotinamide was toxic. Parallel cultures of HCT116 p53+/+ and HCT116 p53−/− of similar low passage number were used throughout.

G_2-M Arrest of Cells Using Nocodazole. For nocodazole release experiments, parallel cultures of p53+/+ and p53−/− cells were seeded at 2×10^6 cells/100-mm dish. Cells were treated 40-h postseeding with 0.2 μg/ml nocodazole for 18 h (as described in Ref. 12). For reversibility studies, the cells were subsequently washed with PBS to remove nocodazole, followed by incubation in fresh medium at 37°C for various times before harvesting by

Received 2/20/03; revised 7/23/03; accepted 7/30/03.

The costs of publication of this article were defrayed in part by the payment of page charges. This article must therefore be hereby marked *advertisement* in accordance with 18 U.S.C. Section 1734 solely to indicate this fact.

[1] Supported by a Yorkshire Cancer Research project grant (to J. M.).

[2] To whom requests for reprints should be addressed, at University of York, Department of Biology, Area 14, YCR P53 Research Group, York Y010 5DD, United Kingdom. Phone: 44-1904-328620; Fax: 011-44-1904-328622; E-mail: ajm24@york.ac.uk.

freeze-thaw for analysis by flow cytometry and lysate preparation for immunoblotting.

Flow Cytometry. Cells were harvested for flow cytometry by the freeze-thaw procedure as described previously (13). The DNA content and antibody staining of cell samples were measured using a Becton Dickinson FACSCalibur (10,000 events/sample). Cell cycle gating and analysis were carried out using Cell Quest software. Histogram deconvolution was performed using Cylchred software.

BrdUrd[3] Pulse Chase. To specifically label S phase cells, parallel cultures of p53+/+ and p53−/− cells were exposed to a 2-min pulse of 30 μM BrdUrd 48-h postseeding. The cells were washed three times with PBS before addition of fresh medium and incubation at 37°C. Cells were harvested by trypsinization and fixed with ice-cold 70% ethanol at: 0, 4, 8, 12, and 16 h. Control dishes were harvested and fixed in parallel. For immunological detection of incorporated BrdUrd, cells were treated with 1 N HCl for 15 min at room temperature, washed with PBS three times and incubated for 1 h with α-BrdUrd antibody (IU4; Caltag). After washing, the cells were incubated with FITC-conjugated secondary antibody for 30 min and stained with propidium idodide (10 μg/ml). BrdUrd-labeled cells were analyzed by flow cytometry, and S phase kinetics were determined by estimating the time taken for cells at the start of S phase (BrdUrd positive but with approximately the same DNA content as cells in G_1 phase) to reach the end of S phase (BrdUrd positive but with the same DNA content as cells in G_2-M). The duration of S phase, and the proportion of cells in S phase, were determined by gating of BrdUrd-positive cells and used to calculate cell cycling time.

Preparation of Extracts and Immunoblotting. Cytoplasmic and nuclear extracts (Fig. 1*A*) were prepared using NE-PER cytoplasmic extraction reagent (Pierce), according to the manufacturer's instructions. For analysis of histone H3 modifications, cells were trypsinized at 37°C for 45–60 s, washed twice with ice-cold PBS, and resuspended in 15 μl of chilled lysis buffer per 10^6 cells (150 mM NaCl, 0.5% NP40, 50 mM Tris (pH 8.0), 10 mM sodium butyrate, 1 mM PMSF, 0.5 mg/ml benzamidine, 2 μg/ml aprotinin, and 2 μg/ml leupeptin). To ensure efficient cell lysis, samples were incubated on ice for 30 min, before centrifugation at 13,000 rpm at 4°C. The supernatant was removed, and the insoluble pellet was resuspended in 4× strength Laemmli's buffer (15 μl/10^6 cells), boiled for 10 min, and passed through a 16-gauge needle. Samples were stored at −70°C and reboiled before resolution by 15% SDS-PAGE. Resolved proteins were electroblotted onto nitrocellulose membrane for 1 h at 25 V using the semidry transfer system (Bio-Rad). Antibodies used to detect specific post-translational modifications on histone H3 were: anti-acetyl K9 antibody (Upstate Biotechnology), anti-acetyl K14 antibody (Upstate Biotechnology), anti-acetyl K18 antibody (CST), anti-acetyl K23 antibody (CST), and anti-phospho S10 antibody (CST). Other antibodies used were DO-1 (Oncogene, against p53), 636 (Santa Cruz Biotechnology, against lamin A/C), and C20 (Santa Cruz Biotechnology, against p300). Visualization of bound antibody was by enhanced chemiluminescence (Roche). The intensity of bands was quantitated by the AlphaImager 1200 system (Alpha Innotech Corp.) and AlphaImager 1200i 3.3b software using scanned images with signal outputs within the linear range. Comparative analyses shown in Figs. 3–5 used data obtained from equivalent exposures of the selected modification (*i.e.*, AcK9 or S10P).

RESULTS AND DISCUSSION

The cell lines chosen for this study were isogenic clones of p53+/+ and p53−/− HCT116 epithelial cells. The parental line retains endogenous wild-type p53 and exhibits normal p53 functions in response to genotoxic stress (4, 14). The rates of cell proliferation of the p53+/+ and p53−/− cells were compared by cell counting over a period of 4 days and also by pulse labeling with BrdUrd to determine S phase kinetics (see "Materials and Methods"). In both cases, the results indicate essentially identical growth rates for the two cell clones, with doubling times of ~21 h (data not shown). Similarities between the p53+/+ and p53−/− cells were also maintained under the various experimental conditions described below. Thus, any observed differences in histone modification(s) between the p53+/+ and p53−/− cells cannot be attributed to intrinsic cell cycle differences or rates of proliferation. Additional controls included immunoblots to show nuclear and cytoplasmic levels of p53, p300 (a HAT), and histone H3 in the isogenic cell clones (Fig. 1*A*). Levels of p53 and histone H3 under the conditions of UV irradiation used in this study are also shown (Fig. 1, *B* and *C*). Lamin A/C was included as a reference control in all experiments (see "Materials and Methods"; Fig. 1*D*).

Loss of p53 Has Site-Specific Effects on Histone H3 Acetylation. First, we characterized site-specific acetylation of histone H3 at lysines K9, K14, and K18 (see "Materials and Methods"; the antibody to acetylated K23 gave no signal and was therefore not included). For K9, the constitutive levels of acetylation were low in p53+/+ cells (Fig. 2*A*, *Lane C*) but reproducibly showed a transient UV-inducible response, peaking within 20 min (Fig. 2*A*, *top panel*). In contrast, little, if any, acetylated K9 was detectable in p53−/− cells under either constitutive conditions or after UV irradiation (Fig. 2*A*, *bottom panel*). This indicates that p53 is involved, directly or indirectly, in the regulation of K9 acetylation levels under both constitutive and UV-induced conditions.

Levels of acetylated K14 were also low but, in contrast to K9, showed similar constitutive levels in both p53+/+ and p53−/− cells (Fig. 2*B*, *Lane C*, *top* and *bottom panels*, and equivalence was verified

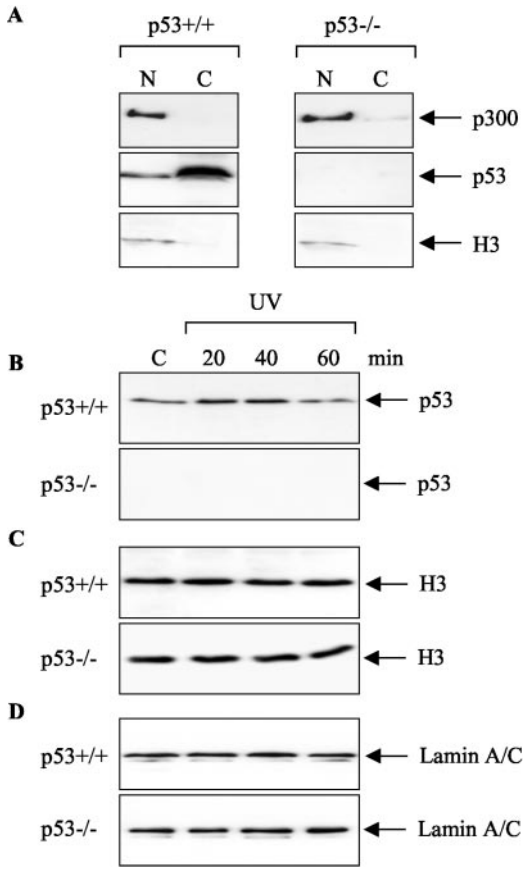

Fig. 1. Comparison of protein levels in isogenic p53+/+ and p53−/− cell clones. *A*, equivalent aliquots of nuclear (*N*) and cytoplasmic (*C*) fractions prepared from parallel cell cultures were immunoblotted for p300, p53, and histone H3 as indicated (see "Materials and Methods"). *B*, relative levels of p53 under normal growth conditions (*C*, constitutive) and at 20, 40, and 60 min after UV irradiation, as indicated ("Materials and Methods"). Histone H3 (*C*) and lamin A/C (*D*) levels. Note that different batches of anti-H3 antibody were used in *A* and *C*; all subsequent anti-histone H3 blots used the same antibody batch as that used for *C*.

[3] The abbreviations used are: BrdUrd, bromodeoxyuridine; CST, Cell Signaling Technology; HAT, histone acetyltransferase; HDAC, histone deacetylase; TFIID, transcription factor IID; TSA, trichostatin A.

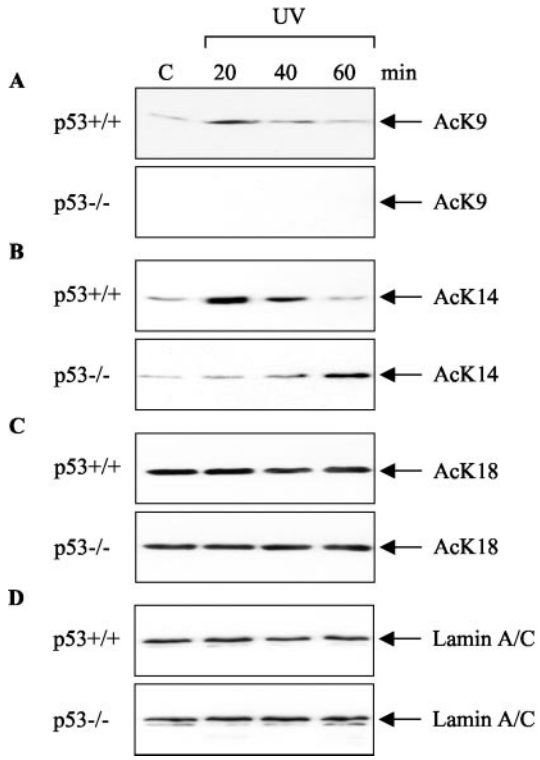

Fig. 2. Site-specific modifications in histone H3 in p53+/+ and p53−/− cells under normal cell growth conditions (*C*) and at different times after UV irradiation as indicated. Paired panels *A–C* represent immunoblots for acetylated K9 (AcK9), AcK14, and AcK18, respectively. *D*, lamin A/C used as internal loading control. Equivalent exposures are presented for each pair of p53+/+ and p53−/− immunoblots shown here and also in Figs. 3 and 4.

by densitometry). Thus, regulation of K14 acetylation appears to be independent of p53 under normal growth conditions. However, a regulatory role for p53 governing acetylation at this site was evident in the response to UV irradiation, which showed delayed kinetics in the p53−/− cells compared with p53+/+ cells (Fig. 2*B*, *bottom panel* cp. *top panel*). Thus, p53 appears to facilitate the transient increase in acetylated K14 observed in response to UV irradiation. K18 differed from both K9 and K14 in that the constitutive levels of acetylated K18 were high and showed little change after UV irradiation, nor between p53+/+ and p53−/− cells (Fig. 2*C*). Acetylation of K18 thus appears to be independent of p53 under the above conditions.

These results demonstrate differential regulation of histone H3 acetylation at lysines K9, K14, and K18 in p53+/+ human epithelial cells under normal growth conditions. Site-specific responses to UV irradiation are also evident at K9 and K14 but not at K18. Loss of p53 correlates with abnormal acetylation at K9 and K14, whereas K18 is unaffected. Thus, p53 appears to be selectively involved in the regulation of histone H3 acetylation at K9 and K14 in human epithelial cells. It is already established that acetylation at K9 and K14 of histone H3 is associated with the relaxation of chromatin for transcription (reviewed in Ref. 15), whereas acetylation at K18 is not similarly involved. This raises the possibility that site-specific effects at K9 and K14 of histone H3 may be mechanistically involved in the ability of p53 to transactivate gene expression in response to UV-induced DNA damage and other forms of genotoxic stress. Coactivator-mediated histone modification is important in transcriptional activation, and recent mutagenesis experiments indicate that acetylation of histone H3 K9 and K14 is important for recruitment of TAFII250, a component of TFIID, to the IFN-β promoter (Ref. 16; reviewed in Ref. 5). Such elegant studies raise the exciting possibility of specific acetylation codes for specific genes, and it will be interesting to apply the same experimental principles to analyze the requirements for coactivator binding at p53-inducible promoters.

Effects of Inhibitors of Histone Deacetylation. Histone acetylation/deacetylation is dynamic and governed by HATs (*e.g.*, p300) and HDACs. As many as 17 HDACs may exist in human cells and are classified on the basis of yeast homologies (17). Classes I and II are sensitive to inhibition by TSA, whereas class III (the Sir2 family) is TSA resistant but sensitive to nicotinamide (18–20). We next used TSA to further characterize the regulation of histone H3 acetylation under normal conditions of cell growth and in response to UV irradiation.

Levels of acetylated K9 increased dramatically after overnight treatment with TSA (Fig. 3*A*), indicating that class I or II HDACs operate at this site. The accumulation of acetylated K9 in the presence of TSA was linear up to 20 h (data not shown) by which time there was an increase of some 26-fold relative to the untreated control cells (Fig. 3*A*, *Lane TSA* + cp. *Lane C*, and Fig. 3*E*). Significantly, the levels of accumulated acetylated K9 were equivalent in both p53+/+ and p53−/− cells (Fig. 3*A*, *Lane TSA* +, *top* and *bottom panels*, and Fig. 3*E*) demonstrating that HAT activity is functional at K9 in p53−/− cells and apparently normal despite the absence of p53. Because the levels of HAT activity at K9 are approximately the same in the p53+/+ and p53−/− cells, it follows that the absence of detectable acetylated K9 in p53−/− cells (Fig. 3*A*, *Lane C*, and Fig. 2*A*, *bottom panel*) must be due to excessive deacetylation at this residue. It also follows that, in p53+/+ cells, the presence of p53 must somehow suppress K9 deacetylation (directly or indirectly) and that this is necessary to maintain constitutive levels of acetylated K9 under normal growth conditions.

However, more complex mechanisms are also evident. This is apparent in unexpected differences, observed between p53+/+ and p53−/− cells, in K9 acetylation after combined treatment with TSA and UV irradiation. In p53+/+ cells, this combined treatment had no additive effect on acetylated K9 levels (Fig. 3*A*, *top panel*; Fig. 3*E*), indicating that UV irradiation does not increase acetyl transferase activity at K9 because such an effect would enhance the overall accumulation of acetylated K9 in the presence of TSA. However, in p53−/− cells, TSA and UV irradiation induced a massive additive effect, with very high accumulation of acetylated K9 (Fig. 3*A*, *bottom panel*, *Lanes 20*, *40*, and *60 min post UV* + *TSA* and Fig. 3*E*). This indicates that, in the absence of p53, UV irradiation causes increased acetyl transferase activity at K9. Alternatively, UV may inhibit deacetylation of K9, but this seems unlikely because no evidence for such an effect is observed in the controls (*i.e.*, in the absence of TSA; see Fig. 2, *Panel A*). No similar additive effect of TSA and UV on K9 acetylation is observed in p53+/+ cells (see above), and we suggest that p53 may directly or indirectly down-regulate UV-induced acetyl transferase activity at K9. Such an effect may prevent abnormally high accumulation of globally acetylated K9 and thus enable more precise regulation of histone modification at sites relevant to the cellular stress response. Evidence for regulatory interplay between p53 and HATs and deacetylases is already established in relation to stress-induced activation of p53 as a transcription factor (21–27). Our present observations now identify p53-dependent, site-specific modifications of histone H3 as possible downstream mediators of the cellular p53 stress response.

In contrast to K9, prolonged exposure to TSA had little or no effect on K14 and K18 acetylation levels (Fig. 3, *B* and *C*, respectively, compare *Lane TSA*+ with *Lane C*). This might be explained if class III deacetylases operate at K14 and K18 of histone H3. To explore this possibility, we repeated the above experiments using nicotinamide in place of TSA ("Materials and Methods"). Nicotinamide blocks TSA-

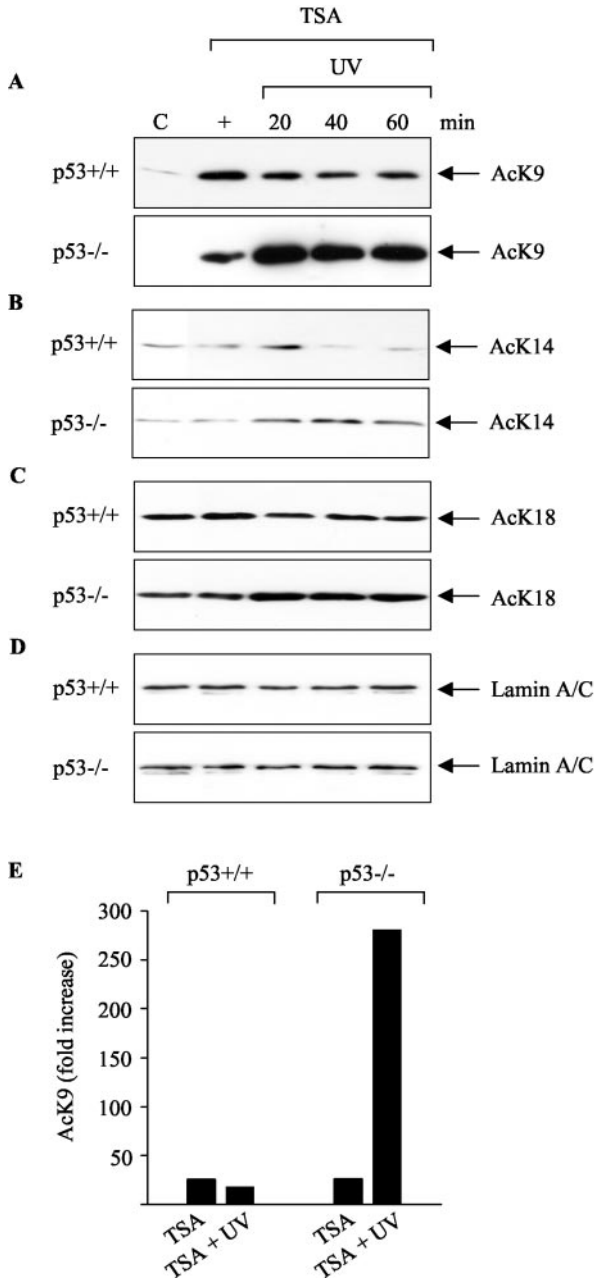

Fig. 3. Effects of TSA, in the presence and absence of UV irradiation, on site-specific acetylation of histone H3 in p53+/+ and p53−/− cells. Paired panels *A–D* as indicated. *E*, histogram showing increases in AcK9 in response to TSA or to TSA plus 20-min UV irradiation calculated by densitometry relative to AcK9 in p53+/+ cells under normal growth conditions. *Lane C*, normal growth conditions; *Lane +*, TSA-treated 20 h. Treatment with TSA plus UV irradiation as indicated.

resistant class III deacetylases and is also reported to stabilize acetylated p53 (21, 26). However, we were unable to demonstrate any effect of nicotinamide on levels of acetylated p53 nor on histone H3 acetylation status under the conditions of our experiments (data not shown). Thus, the possible role of class III deacetylases at K14 and K18 of histone H3 remains to be established.

Abnormal Phosphorylation of Histone H3 at Serine 10 in p53−/− Cells. Phosphorylation at serine 10 was included in this study because this is an important and highly conserved modification of histone H3. S10 phosphorylation occurs at G_2-M of the cell cycle and determines proper chromosome condensation and segregation and also normal chromosome dynamics (6–10). It follows that the regulation of S10 phosphorylation is crucial in eukaryotic cells. In *Saccharomyces cerevisiae* and *Caenorhabditis elegans*, the balance of S10 phosphorylation is determined by opposing activities of Ipl/aurora kinase and its genetically interacting phosphatase Glc7/PPI (8). In human cells, a related kinase, AIM/aurora B, is implicated (12). We now present evidence that loss of p53, normally important for the maintenance of genomic integrity in mammalian cells, profoundly affects the balance of histone H3 phosphorylation at S10 in human epithelial cells.

Analysis of p53+/+ cells demonstrated that the level of phosphorylated S10 observed under normal growth conditions showed little, if any, increase after exposure of the cells to UV irradiation (Fig. 4*A*, *left panel*). Similarly, treatment with TSA, in the presence or absence of UV irradiation, had no obvious effect on S10 phosphorylation in

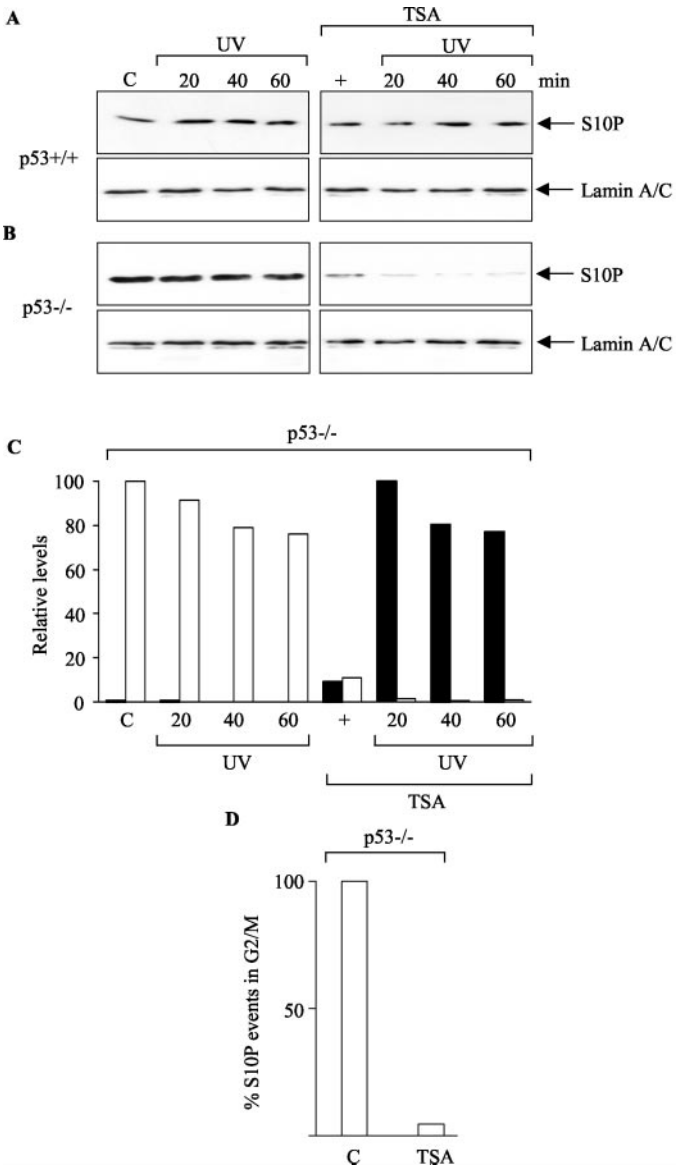

Fig. 4. Levels of phosphorylated S10 (*S10P*) in p53+/+ and p53−/− cells and effects of treatment with UV irradiation, with TSA and TSA plus UV irradiation. *A* and *B*, S10P immunoblots of equivalent samples of p53+/+ and p53−/− cells, respectively. Experimental treatments were as indicated: *C*, normal growth conditions; +, TSA alone. *C*, histogram showing relative changes in AcK9 and S10P in p53−/− cells after treatment with UV irradiation and/or TSA as indicated; changes in AcK9 were calculated relative to highest AcK9 value (TSA plus 20 min UV) and S10P relative to highest S10P value (normal growth conditions). ■, AcK9; □, S10P. *D*, quantitative comparison of cell cycle gated fractions of G_2-M cells positive for S10P determined by fluorescence-activated cell sorter analysis after growth under normal conditions (*C*) or after 20-h treatment with TSA as indicated; total G_2-M cells = 3700 and 5000, respectively.

p53+/+ cells (Fig. 4*A*, *right panel*). Thus, in p53+/+ cells, S10 phosphorylation levels appear constant under conditions which induce marked changes in histone H3 acetylation (see Figs. 2, *A* and *B* and 3*A*). In the absence of p53, however, a very different picture emerged. First, abnormally high levels of phosphorylated S10 were observed in p53−/− cells compared with p53+/+ cells under normal growth conditions (Fig. 4*B*; ~4-fold higher in p53−/− cp. p53+/+ cells as determined by densitometry). UV irradiation had no effect on these levels (Fig. 4*B*, *left panel*). TSA, on the other hand, had marked and completely unexpected effects. TSA alone caused a 10-fold reduction in phosphorylated S10 relative to the untreated control (Fig. 4*B*, *Lane TSA +*, *right panel*) and TSA treatment in combination with UV irradiation resulted in almost complete loss of phosphorylated S10 (Fig. 4*B*, *right panel*). Loss of phosphorylated S10 was confirmed for G_2-M cells using flow cytometry (see Fig. 4*D*).

The unexpected effects of TSA on both histone H3 acetylation and phosphorylation in p53−/− cells may have major significance in the context of anticancer therapy. HDAC inhibitors are currently being developed as anticancer agents, and the first clinical trials are already in place (28). Remarkably, however, the basis of selective cytotoxicity of HDAC inhibitors for tumor cells has remained a mystery. The biochemical effects of inhibitors of HDACs are likely to be complex and involve both histone and nonhistone proteins. Moreover, cell diversity and compensatory feedback pathways may further confound attempts to elucidate the mechanism by which HDAC inhibitors are able to reduce the growth of tumor cells and/or induce apoptosis. By comparing isogenic clones of cells derived from a colorectal carcinoma, we now identify p53-related differences in the effects of HDAC inhibition by TSA. In particular, we show that TSA can cause unexpected abnormalities in S10 phosphorylation and that this effect is specific for p53-deficient cells, thus identifying a potential mechanism by which inhibitors of histone deacetylation may selectively affect the viability of tumor cells lacking normal p53 functions. This raises the possibility that, although both p53-positive and p53-deficient tumors are sensitive to HDAC inhibitors, the pathways involved in tumor suppression may differ depending on p53 status (wild type or deficient; latent or activated). Such considerations may contribute toward our eventual understanding of tumor growth suppression in response to inhibitors of histone deacetylation.

Why should TSA, a highly selective inhibitor of histone deacetylation (29), also affect histone phosphorylation? The simplest explanation is that stabilization of acetylated K9 (Fig. 3*A*) suppresses phosphorylation at the adjacent S10 residue. However, no evidence for such an effect was observed in p53+/+ cells in which levels of phosphorylated S10 remained constant despite a 26-fold accumulation of acetylated K9 in the presence of TSA (see Fig. 4*A* for S10 phosphorylation and Fig. 3*A* for K9 acetylation; *Lanes C* and *TSA+*). In contrast, equivalent accumulation of acetylated K9 in p53−/− cells was associated with a loss of phosphorylated S10 (Figs. 3*A* and 4*B*). Indeed, remarkable reciprocity between acetylated K9 and phosphorylated S10 was evident in the p53−/− cells under all conditions tested (Fig. 4*C*).

Loss of p53 Affects Recovery of Cells from G_2-M Arrest. Phosphorylation of histone H3 S10 occurs mainly in G_2-M of the cell cycle. To study the effects of p53 on phosphorylation of histone H3 in more detail, we next used the reversible inhibitor nocodazole to arrest cells in G_2-M of the cell cycle. After 18-h treatment with nocodazole, the accumulation of cells in G_2-M was essentially equivalent for the p53+/+ and p53−/− cells (64.8 and 66.2% cells in G_2-M, respectively; Fig. 5). Aliquots of the nocodazole-treated cells were analyzed for S10P by immunoblotting, and, as expected, the accumulation of G_2-M cells correlated with high levels of S10P (Fig. 5). Thus, by these criteria, the p53+/+ and p53−/− cells appear equally sensitive to the

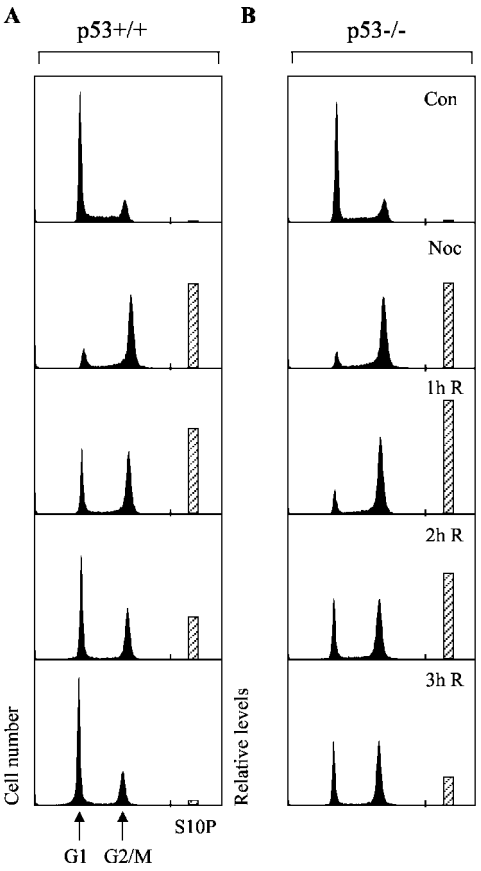

C **p53+/+ cells**

	Con	Noc	1h R	2h R	3h R
G1	51.4	11.6	27.0	44.9	59.1
S	32.7	23.7	26.6	15.2	18.2
G2/M	15.9	64.8	46.3	39.9	22.7

D **p53-/- cells**

G1	54.3	8.6	11.1	27.9	28.0
S	28.8	25.3	21.3	19.8	18.2
G2/M	16.8	66.2	67.6	52.3	53.8

Fig. 5. Effects of nocodazole treatment and its removal on the cell cycle and on phosphorylated levels of S10 of histone H3 in p53+/+ and p53−/− cells. *A* and *B*, comparison of cell cycle profiles of p53+/+ cells and p53−/− cells, respectively, after treatment with 0.2 μg/ml nocodazole for 18 h (*Noc*) and at various time points after the removal (*R*) of nocodazole as indicated. *Con*, cells grown under normal conditions. ▨, histograms showing the relative levels of phosphorylated S10 (*S10P*) in equivalent amounts of extract prepared from confluent cells, as calculated by densitometry of immunoblots. *C* and *D*, relative proportions of G_1, S, and G_2-M phase cells in each population of p53+/+ and p53−/− cells, respectively, as determined by histogram deconvolution.

effects of nocodazole. However, clear differences were apparent after removal of the inhibitor. For the p53+/+ cells, the G_2-M levels fell progressively from ~65 to 22% by 3 h after removal of nocodazole (Fig. 5, *left panels*). This apparent recovery in cell cycling was paralleled by a progressive decrease in S10P levels (Fig. 5; histograms in *left panels*). In contrast, the p53−/− cells showed a much slower and incomplete recovery from the nocodazole-induced G_2-M arrest, together with sustained elevation of S10P levels (Fig. 5; *right panels*). Failure to revert to a normal cell cycle profile might be explained by a deficiency in the ability to reorganize chromatin structure in the p53−/− cells. Furthermore, any such deficiency may be causally linked with abnormal regulation of S10P levels.

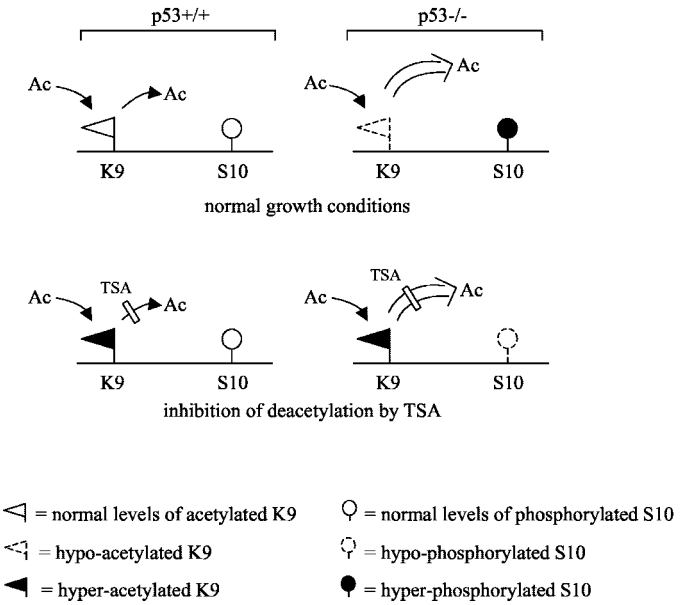

Fig. 6. Schematic indicating the abnormally high, constitutive deacetylation of K9 in p53−/− cells and the abnormal reciprocity between AcK9 and S10P in the presence and absence of TSA.

Using isogenic cell clones, we have now demonstrated p53-related abnormalities in S10 phosphorylation by two independent approaches: (*a*) by treatment with TSA plus UV irradiation (Fig. 3, *A* and *E*); and (*b*) during the recovery of cells from nocodazole-induced G_2-M cell growth arrest (Fig. 5). Histone H3 S10 phosphorylation is tightly associated with chromatin condensation/segregation during G_2-M (6–10) and is important for the maintenance of ploidy (12). We suggest that any p53-related abnormality in S10 phosphorylation may contribute toward the development of aneuploidy in p53-deficient cancers, thereby favoring malignant progression.

Our overall observations on K9 and S10 are summarized in Fig. 6. We conclude that: (*a*) in p53+/+ cells, the presence of p53 in some way modulates reciprocity between levels of acetylation at K9 and phosphorylation at S10; and (*b*) this novel p53 function is necessary for the normal regulation of S10 phosphorylation. In the absence of p53, wide variations in phosphorylated S10 inversely correlate with levels of acetylated K9 (Fig. 4*C*). Thus, the reduced levels of acetylated K9 observed in p53-deficient human cells (this study; Fig. 2*A*) may account for the observed elevation in phosphorylated S10 in p53−/− cells under normal growth conditions (Fig. 4).

In summary, our work indicates that loss of p53 has site-specific effects on histone H3 modifications. In particular, we show that loss of p53, directly or indirectly, perturbs the normal regulation of S10 phosphorylation. We suggest that this effect may contribute toward the development of abnormal chromosomes and aneuploidy in p53-deficient cancers.

ACKNOWLEDGMENTS

We thank Bert Vogelstein for making available the isogenic clones of HCT116 p53+/+ and p53−/− cells.

REFERENCES

1. Vogelstein, B., Lane, D. P., and Levine, A. J. Surfing the p53 network. Nature (Lond.), *408:* 307–310, 2000.
2. Rubbi, C. P., and Milner, J. p53 is a chromatin accessibility factor for nucleotide excision repair of DNA damage. EMBO J., *22:* 975–986, 2003.
3. Ramanathan, B., and Smerdon, M. J. Changes in nuclear protein acetylation in UV-damaged cells. Carcinogenesis (Lond.), *7:* 1087–1094, 1986.
4. Bunz, F., Hwang, P. M., Torrance, C., Waldman, T., Zhang, Y., Dillehay, L., Williams, J., Lengauer, C., Kinzler, K. W., and Vogelstein, B. Disruption of p53 in human cancer cells alters the responses to therapeutic agents. J. Clin. Investig., *104:* 263–269, 1999.
5. Iizuka, M., and Smith, M. M. Functional consequences of histone modifications. Curr. Opin. Genet. Dev., *13:* 154–160, 2003.
6. Hooser, A. V., Goodrich, D. W., Allis, C. D., Brinkley, B. R., and Mancini, M. A. Histone H3 phosphorylation is required for the initiation, but not the maintenance, of mammalian chromosome condensation. J. Cell Sci., *111:* 3497–3506, 1998.
7. Wei, Y., Yu, L., Bowen, J., Gorovsky, M. A., and Allis, C. D. Phosphorylation of histone H3 is required for proper chromosome condensation and segregation. Cell, *97:* 99–109, 1999.
8. Hsu, J-Y., Sun, Z. W., Li, X., Reuben, M., Tatchell, K., Bishop, D. K., Grushcow, J. M., Brame, C. J., Caldwell, J. A., Hunt, D. F., Lin, R., Smith, M. M., and Allis, C. D. Mitotic phosphorylation of histone H3 is governed by Ip1/aurora kinase and Glc7/PPI phosphatase in budding yeast and nematodes. Cell, *102:* 279–291, 2000.
9. Hendzel, M. J., Wei, Y., Mancini, M. A., Van Hooser, A., Ranalli, T., Brinkley, B. R., Bazett-Jones, D. P., and Allis, C. D. Mitosis-specific phosphorylation of histone H3 initiates primarily within pericentromeric heterochromatin during G_2 and spreads in an ordered fashion coincident with chromosome condensation. Chromosoma (Berl.), *106:* 348–360, 1997.
10. Giet, R., and Glover, D. M. *Drosophila* aurora B kinase is required for histone H3 phosphorylation and condensin recruitment during chromosome condensation and to organise the central spindle during cytokinesis. J. Cell Biol., *152:* 669–682, 2001.
11. Stock, R. P., and Bialy, H. The sigmoidal curve of cancer. Nat. Biotechnol., *21:* 13–14, 2003.
12. Ota, T., Suto, S., Katayama, H., Han, Z. B., Suzuki, F., Maeda, M., Tanino, M., Terada, Y., and Tatsuka, M. Increased mitotic phosphorylation of histone H3 attributable to AIM-1/aurora B overexpression contributes to chromosome number instability. Cancer Res., *62:* 5168–5177, 2002.
13. Milner, J., and Watson, J. V. Addition of fresh medium induces cell cycle and conformation changes in p53, a tumour suppressor protein. Oncogene, *5:* 1683–1690, 1990.
14. Zhang, L., Yu, J., Park, B. H., Kinzler, K. W., and Vogelstein, B. Role of Bax in the apoptotic response to anti-cancer agents. Science (Wash. DC), *290:* 989–992, 2000.
15. Jenuwein, T., and Allis, C. D. Translating the histone code. Science (Wash. DC), *293:* 1074–1079, 2001.
16. Agalioti, T., Chen, G., and Thanos, D. Deciphering the transcriptional histone acetylation code for a human gene. Cell, *111:* 381–392, 2002.
17. Gray, S. G., and Eckstrom, T. J. The human histone deacetylase family. Exp. Cell Res., *262:* 75–83, 2001.
18. Landry, J., Sutton, A., Tafrov, S. T., Heller, R. C., Stebbins, J., Pillus, L., and Sternglanz, R. The silencing protein SIR2 and its homologs are NAD-dependent protein deacetylases. Proc. Natl. Acad. Sci. USA, *97:* 5807–5811, 2000.
19. Guarente, L. Sir2 links chromatin silencing, metabolism and aging. Genes Dev., *14:* 1021–1026, 2000.
20. Shore, D. The Sir2 protein family: a novel deacetylase for gene silencing and more. Proc. Natl. Acad. Sci. USA, *97:* 14030–14032, 2000.
21. Luo, J., Nikolaev, A. Y., Imai, S., Chen, D., Su, F., Shiloh, A., Guarente, L., and Gu, W. Negative control of p53 by Sir2α promotes cell survival under stress. Cell, *107:* 137–148, 2001.
22. Avalos, J. L., Celic, I., Muhammad, S., Cosgrove, M. S., Boeke, J. D., and Wolberger, C. Structure of a Sir2 enzyme bound to an acetylated p53 peptide. Mol. Cell, *10:* 523–535, 2002.
23. Juan, L. J., Shia, W. J., Chen, M. H., Yang, W. M., Seto, E. Lin, Y. S., and Wu, C. W. Histone deacetylases specifically down-regulate p53-dependent gene activation. J. Biol. Chem., *275:* 20436–20443, 2000.
24. Murphy, M., Ahn, J., Walker, K. K., Hoffman, W. H., Evans, R. M., Levine, A. J., and George, D. L. Transcriptional repression by wild-type p53 utilises histone deacetylases, mediated by interaction with mSin3a. Genes Dev., *13:* 2490–2501, 1999.
25. Vaziri, H., Dessain, S. K., Ng Eaton, E., Imai, S. I., Frye, R. A., Pandita, T. K., Guarente, L., and Weinberg, R. A. hSIR2^{SIRT1} functions as an NAD-dependent p53 deacetylase. Cell, *107:* 149–159, 2001.
26. Langley, E., Pearson, M., Faretta, M., Bauer, U. M., Frye, R. A., Minucci, S., Pelicci, P. G., and Kouzarides, T. Human SIR2 deacetylates p53 and antagonises PML/p53-induced cellular senescence. EMBO J., *21:* 2383–2396, 2002.
27. Barlev, N. A., Liu, L., Chehab, N. H., Mansfield, K., Harris, K. G., Halazonetis, T. D., and Berger, S. L. Acetylation of p53 activates transcription through recruitment of co-activators/histone acetyltransferases. Mol. Cell, *8:* 1243–1254, 2001.
28. Marks, P. A., Richon, V. M., Breslow, R., and Rifkind, R. A. Histone deacetylase inhibitors as new cancer drugs. Curr. Opin. Oncol., *13:* 477–483, 2001.
29. Yoshida, M., Kijima, M., Akita, M., and Beppu, T. J. Potent and specific inhibition of mammalian histone deacetylase both *in vivo* and *in vitro* by trichostatin A. J. Biol. Chem., *265:* 17174–17179, 1990.

Loss of p53 Has Site-Specific Effects on Histone H3 Modification, Including Serine 10 Phosphorylation Important for Maintenance of Ploidy

Simon J. Allison and Jo Milner

Cancer Res 2003;63:6674-6679.